LIVE/DEAD CELL ASSAY BASED ON DIELECTROPHORESIS-ON-A-CHIP

Ciprian ILIESCU[1], Guillaume TRESSET [2] Florina S. ILIESCU[3], Paul E. STERIAN[4]

Articolul prezimtă o metodă de separare a populațiilor de particule prin dielectroforeză pe cip (DEP) cu electrozi asimetrici sub curgere continuă. Structura dispozitivului DEP (cu un electrod gros care defineşte pereții canalului microfluidic şi un electrod subțire), ca şi fabricarea şi caracterizarea dispozitivului au fost descrise anterior. O caracteristică a acestei structuri este că generează un gradient crescut al câmpului electric în plan vertical în care pot levita particulele care posedă DEP negativă. Metoda de separare constă în captarea în partea de jos a canalului microfluidic a populației având comportare DEP pozitivă, în timp ce populația care prezintă DEP negativă este antrenată spre ieşire prin curgere. Celulele vii şi moarte ale drojdiei de bere au fost utilizate pentru testarea metodei de separare.

The paper presents a field-flow separation method of particle populations in a dielectrophoretic (DEP) chip with asymmetric electrodes under continuous flow. The structure of the DEP device (with one thick electrode that defines the walls of the microfluidic channel and one thin electrode), as well as the fabrication and characterization of the device were previous described. A characteristic of this structure is that it generates an increased gradient of electric field in the vertical plane that can levitate the particles experiencing negative DEP. The separation method consists of trapping one population to the bottom of the microfluidic channel using positive DEP, while the other population that exhibits negative DEP is levitated and flowed out. Viable and nonviable yeast cells were used for testing the separation method.

Keywords: BioMEMS; Dielectrophoresis; Cell separation; Microfluidics

1. Introduction

Neutral particles can be manipulated using non-uniform electric field; the phenomenon is called dielectrophoresis (DEP). The force $\mathbf{F}_{\mathbf{DEP}}$ that generates the

[1] PhD., Institute of Bioengineering and nanotechnology, Singapore, e-mail: ciliescu@ibn.a-star.edu.sg
[2] PhD, CNRS, Laboratoire de Physique des Solides, University Paris-Sud, Orsay, France, e-mail : tresset@lps.u-psud.fr
[3] M.D, Republic Polytechnic, Singapore, e-mail: florina_iliescu@rp.sg
[4] Prof., Physics Department, University POLITEHNICA of Bucharest, Romania

movement is strongly dependent on the gradient of the electric field. According to the methods used for achieving this gradient, different solutions were proposed. Travelling wave DEP is the method of changing the phase of the applied electric field [1, 2]. Another method - "isolating DEP"- consists of generating gradient of electric field using of non-homogenous dielectric medium between two parallel electrodes [3, 4]. Chiou *et al* proposed a DEP device where the gradient of the electric field is generated using an optical image on a photodiode surface [5]. Moving DEP, presented in [6] by Kua *et al* is a method where particles, initially trapped using a non-uniform electric field, are moved using a travelling electric field. In the last method, the gradient of the electric field is generated by the non-uniform shape of the electrodes. These electrodes can be thin films [7, 8], 3D pillars [9, 10], 3D electrodes that simultaneously define the microfluidic channel [11] or even a combination between a thin electrode and a 3D electrode [12].

According to their complex permittivity relatively to the medium, the particles can move towards the regions with higher field strength ("positive DEP") or towards regions with low electric field strength ("negative DEP"). Trapping of the particles in different regions of DEP device using positive and negative DEP together with hydrodynamic (Stokes) forces that act on the particles were used in microfluidic devices for separation of different cell or particle populations [13-15]. In previous work [16-18] we described different separation techniques in DEP devices with 3D electrodes.

Here, we report a field-flow separation technique under continuous flow in DEP chip with asymmetric electrodes (one bulk and one thin). The fabrication process of the DEP device and its application on cell trapping was described in a previous work [12]. The separation method consists of trapping one population using positive DEP in the plane of the thin electrode, while the other population is levitated (using negative DEP) and flowed out. A characteristic of the device is a strong vertical DEP force (for negative DEP) that levitates the particles. Other advantages of the device are: a completely enclosed design, a small working volume (around 1 mL) and small dimensions of the chip (4x12 mm).

2. Device description and fabrication

A schematic view of the structure of the DEP device is presented in Figure 1. A structure with heavy doped silicon (single crystal) pillars (100-µm-thick) is bonded between two glass dies which assure the ceiling and the floor of the microfluidic channel. On the bottom glass die, the thin electrodes are defined in a 1-µm-thick amorphous silicon layer (heavy doped). The 100-µm-thick die presents metalized via-holes which allow the contact of the independent electrodes defined in the thick and thin silicon material. The top glass die presents two holes as the inlet/outlet of the solution with populations of particles.

The fabrication method was in detail described in [12]. A 100-µm-thick heavy doped silicon wafer is anodically bonded on a Corning 7740 glass wafer using an EVG520 wafer bonding system. The bonding was performed in vacuum at 305OC (the temperature on which the silicon and the glass exhibit the same expansion [19]) using an applied force of 500N and an applied voltage of 1000V. The current was limited at 10mA and the process was stop when the value of current was 4mA. This "incomplete" anodic bonding process aloud performing of a second anodic bonding process (glass remains conductive at temperature above 400^{O}C) [11]. The glass wafer presents drilled holes for inlet/outlet holes of the microfluidic device. The thick electrodes are defined using a classical deep reactive ion etching (RIE, Bosch process) in the silicon layer (Figure 2a) on ICP Deep RIE system (Alcatel 101) through a 1µm-thick PECVD SiO2 mask. Before the anisotropic etching of the silicon, the bonded structure was attached using wax to a dummy silicon wafer. The defined silicon structure is in the same time electrode and defines the walls of the microfluidic channel. On a second glass wafer the thin electrodes are performed using RIE on a thin amorphous Si layer (heavy doped with aluminum) – Figure 2b. Amorphous silicon layer (2.5µm-thick) was used as material for the thin electrode due to the fact that it is a good "etch-stop" layer in highly concentrated HF solution, being often used as masking layer for deep wet etching of glass [20]. The stress value in the thin amorphous silicon layer is very important. The thin electrode will be contacted through a viaholes fabricated through the glass using a wet etching process. The wet etching process will stop on the amorphous silicon layer and will generate a membrane.

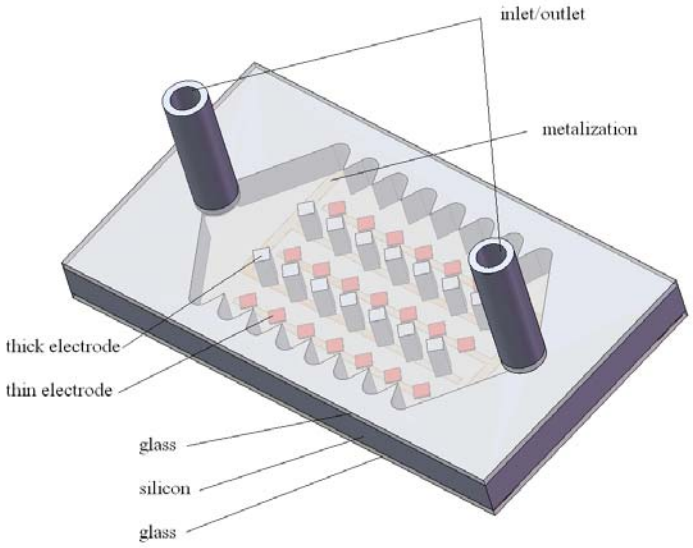

Fig. 1. 3D view of the DEP chip with asymmetric electrodes.

Even the diameter of the membrane is not very big (around 100 µm), a low value of the stress is desired. The stress was controlled by annealing process [21] (the final value was around 150 MPa compressive from an initial value of 500MPa compressive). Must be mention that a compressive stress is desired comparing with a tensile value (the tensile stress tends to broke the membrane - similar considerations are presented in [22]). After aligning the wafers with the electrodes, a second anodic bonding process (at 450^{O}C, with an applied voltage of 1500 V, a force of 1000N in vacuum) assures the sealing of the structure with microfluidic channel. A chemical polishing process in a HF/HCl solution (10/1) [23] is used for thinning up to a thickness of 100µm the glass wafer with the electrodes- Fig. 2c. Via-holes are performed in the thin glass wafer using a Cr/Au masking layer [24]- Fig. 2d. A metallization, on the glass surface with via-holes, assures the contact between independent electrodes and the connections of the electrodes with the PCB- Fig. 2e.

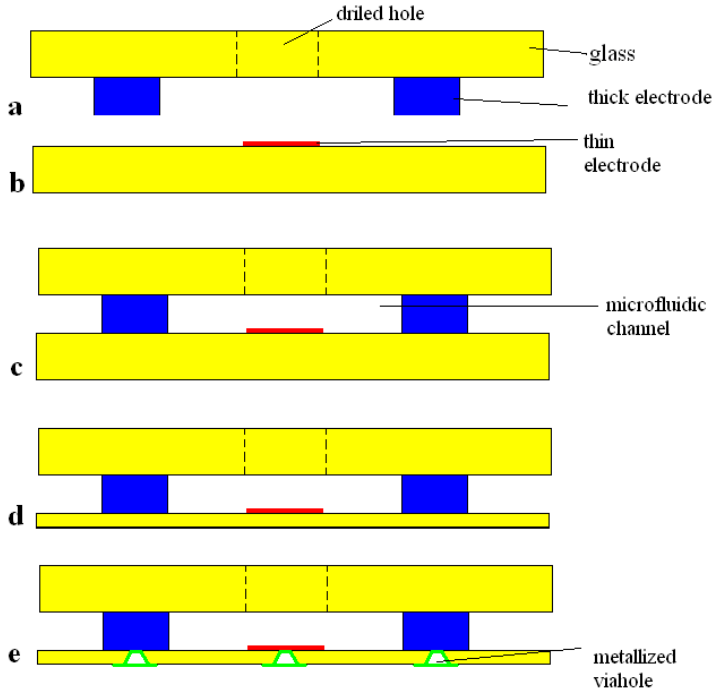

Fig. 2. Fabrication process of the DEP device: (a) Patterning of the thick electrodes, (b) patterning of the thin electrodes, (c) assembling of the wafers using anodic bonding, (d) chemical polishing of the glass wafer (e) fabrication of the metalized viaholes.

3. Separation method

Reviews of the separation techniques using dielectrophoresis detailed description of DEP are presented by Hughes [25] and Gascoyne and Vykoukal [26]. According with the above mentioned papers the separation methods can be summarized as: flow separation, field flow fractionation, stepped flow separation, travel wave dielectrophoresis, and the ratcheting mechanism. Flow separators have been reported in [27] and [28]. The method consists of flowing a particle suspension solution over an electrode array. The population that exhibits positive DEP is trapped near the electrode while the other population is repelled into the center of the chamber to be subsequently pushed by the flow towards the outlet. Another flow separator using 3D arrays of electrodes embedded in microchannels -so-called "deflector" structure (electrodes oriented at certain angle compared with the flow direction) - is presented in [29]. We presented in previous work few dielectrophoretic separation methods in DEP devices with 3D electrodes [16-18]. A characteristic of these methods is that the nonregular shape of the electrodes, used for the generation of the gradient of the electric field, is the source of generation of gradient of fluid velocity. As a results a population –that exhibit negative DEP-is trapped where the velocity of the fluid is low (so-called "dead fluid regions") while the other population (that experience positive DEP) is trapped where the velocity of the fluid is at list with one order increased. The main advantage of these methods is a reduce Joule effect [30]. Another method that uses a fluid velocity gradient to separate particles- known as field-flow fraction- is presented in [31]. Using an applied dielectrophoretic force field, different particles will be located at different regions within the fluid velocity gradient and will travel with different velocities. Sorting of live and dead yeast cells using a 3D electro-mechanical filter under continuous flow is presented in [32, 33]. Separation of white and red blood cells is presented in [34, 35].A vertical flow is obstructed by a 1mm-thick 3D filter build from 100μm-diameter silica particles sandwiched between mesh electrodes using a glass frame. Cells exhibiting positively DEP trapped around the contact points between the silica beads while the other cell population is repelled into the space between silica beads a flown out.

The proposed separation method is illustrated in Fig. 3. The mixture with two particle populations is flowed through the microfluidic device. The magnitude of the electric field, its frequency and the medium properties are selected in such a way that one population exhibits positive DEP while the other one negative DEP.

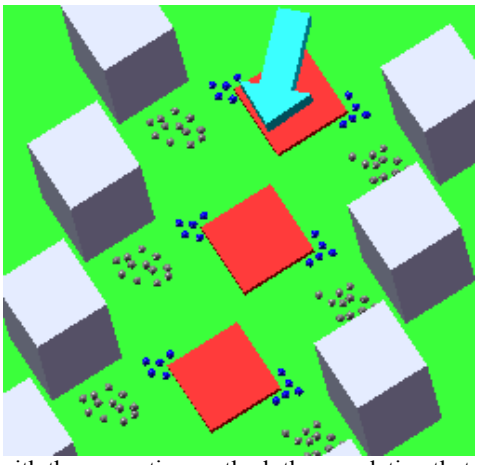

Fig. 3. Schematic view with the separation method: the population that exhibits positive DEP is trapped on the bottom of the device, while the population that experiences negative DEP is levitated and flowed out.

Applying the electric field under continuous flow the particles that exhibit negative DEP are levitated due to a strong DEP force in a vertical direction that overcome the buoyancy force while the particles that experience positive DEP are collected on the bottom of the device in the vicinity of the thin electrode. As a result the population that experiences negative DEP will be collected at the outlet. Releasing the electric field and increasing the flow in the microfluidic channel, the second population is collected at the outlet.

4. Analytical considerations

We established a hydrodynamic model of particle trajectory in order to identify the factors that govern the separation mechanisms. The movement of a particle in a fluid influenced by $\mathbf{F}_{\mathbf{DEP}}$ is given by:

$$m\frac{d\mathbf{u}}{dt} = -\gamma(\mathbf{u}-\mathbf{v}) + \mathbf{F}_{\mathbf{DEP}} + \mathbf{F}_{\mathbf{B}}, \tag{1}$$

where m denotes the particle mass, $\mathbf{u}$ and $\mathbf{v}$ the particle and fluid velocities respectively, and γ the friction factor of the particle in the fluid, which is expressed by:

$$\gamma = 6\pi\eta a \tag{2}$$

for a spherical particle of radius a with η being the fluid viscosity. $\mathbf{F}_{\mathbf{B}}$ is the buoyancy force oriented along the acceleration of gravity **g**, and expressed by:

$$\mathbf{F}_{\mathbf{B}} = 4/3\,\pi a^3(\rho_p - \rho_m)\mathbf{g} \tag{3}$$

with ρ_p and ρ_m the densities of the particle and the medium respectively. The DEP force scales with the gradient of the squared electric field intensity, [36]:

$$\mathbf{F_{DEP}} = 2\pi a^3 \,\mathrm{Re}[K]\nabla \mathbf{E}^2 \tag{4}$$

where $\mathrm{Re}[K]$ is the real part of the Clausius-Mossotti factor, and depends on the frequency and on the difference of dielectric properties between particle and medium. We consider first the dielectrophoretic force oriented along the vertical z axis. Finite elements calculations presented in a previous report [12] showed that its strength decays exponentially with the distance from the floor, so that we can write as an approximation:

$$F_{DEP}^{z} \approx F_{DEP,0}^{z} \exp(-\zeta z). \tag{5}$$

In the case the particle undergoes a negative DEP, it eventually levitates up to a height where the DEP force balances the buoyancy force, namely:

$$z = 1/\zeta \ln\left(F_{DEP,0}^{z} / F_B\right) \tag{6}$$

At the same time, the particle is trapped in the horizontal plane into a well of minimal electric field. In order to untrap it and collect it at the outlet of the device, a fluid flow of velocity v is applied along the x direction. The condition for untrapping is then:

$$v > \left|F_{DEP}^{x} / \gamma\right| \tag{7}$$

If the particle undergoes a positive DEP, it will get trapped onto the floor of the channel, where the DEP force is the highest and the fluid flow null because the fluid velocity profile is parabolic across the channel. To estimate the trapping timescale, we consider a particle initially at height z_0 with a negligible buoyancy force; note that this force would accelerate the trapping process anyway. The equation of motion Eq. (1) projected onto the vertical axis reads:

$$\frac{m}{\gamma}\frac{d^2 z}{dt^2} = -\frac{dz}{dt} - \frac{F_{DEP}^{0}}{\gamma}\exp(-\zeta z). \tag{8}$$

The first term arising from the inertial force is negligible due to the high frictions exerted to the particle by the viscous fluid so that the DEP force is constantly in equilibrium with the drag force. It results from the integration of Eq. (2) that the time Δt for the particle to travel from z_0 to the floor is given by:

$$\Delta t = \frac{\gamma}{F_{DEP}^{0}\zeta}\left[\exp(\zeta z_0) - 1\right]. \tag{9}$$

Finite elements calculations gave a typical vertical force of 10^{-9} N at the floor level and a length scale $1/\zeta$ of 30 μm. Considering a friction factor of 10^{-7} SI and an initial height of 80 μm which corresponds to the ceil of the device, the trapping time is ~40 ms. Since the fluid actually flows through the channel, the

particle also travels along the x direction. The velocity profile of the fluid is quadratic with a maximum value v_{max} halfway of the channel and vanishes at the walls. The lateral distance Δx travelled by the particle during its trapping is obtained by integration of the velocity profile as the particle moves towards the floor in Δt given by.:

$$\Delta x = \int_0^{\Delta t} v_{\max}\left(1 - \frac{1}{z_0^2}\left(2z(t) - z_0\right)^2\right)dt < \Delta x_{\max} = v_{\max}\Delta t\,. \tag{10}$$

The condition for untrapping imposes a fluid velocity v_{max} of 10^{-3} m.s^{-1} for a lateral DEP force of ~10^{-10} N according to simulations. The upper estimate Δx_{max} is therefore ~40 μm, far smaller than the channel length (a few millimeters) so that all the particles to be trapped can be immobilized within the device.

3. Joule heating effect

The non-uniform shape of the DEP electrodes that generates high electric field generates also a large power density in the fluid between the electrodes. This increased power density associated with the small volume and a bad thermal conductivity of the glass could give rise to a large temperature increase in the solution with suspended particles. The temperature balance equation describes the relationship between the generation and dissipation of heat is presented in [20]:

$$\rho_m c_p \nabla T + \rho_m c_p v \cdot \frac{\partial T}{\partial t} = k\nabla^2 T + \sigma E^2 \tag{11}$$

where c_p is the specific heat at constant pressure, k the thermal conductivity, v the velocity, ρ_m the density, σ the electrical conductivity of the medium. For a capacitor type, this equation is solved in [21] and the variation of temperature can be approximated with the formula:

$$\Delta T \approx \frac{\sigma V_{rms}^2}{k} \tag{12}$$

where V_{rms} is the potential difference across the electrodes. As Ramos et al shows in [21] the Joule heating effect can be ignored for solutions of low conductivity. For biological applications, usually high conductivity buffers must be used (with σ between 0.1 and 1 S m^{-1}) and the risks of achieving temperature of 100^{O}C is quite high.

In order to investigate the thermal distribution and temperature profile within the DEP chip with different types of electrode, finite element analysis tools (ANSYS software) have been used. Simulated pictorial results for the temperature profile of the DEP chip with planar electrodes and asymmetric electrodes are presented in Figure 4a and Figure 4b respectively.

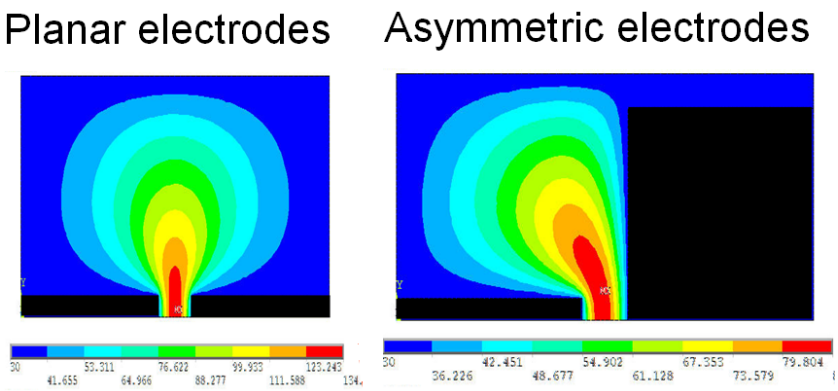

Fig. 4. Simulation of the temperature variation in a DEP structure with planar electrodes and a DEP structure with asymmetric electrodes

To perform the simulations the following parameters are used: applied voltage $V = 20\ V$ *peak-to-peak, t*hermal conductivity of the medium: $k = 0.6\ Jm^{-1}s^{-1}K^{-1}$ and electrical conductivity: $\sigma = 1\ Sm^{-1}$ [27], it is observed that for high conductive solution such as $\sigma = 1\ Sm^{-1}$, the change in temperature (∇T) for the case of planar electrode can reach up to $100^{\circ}C$. Such high temperature will destroy the biological sample. However, under the same conditions, for the case of 3D electrode (shown in [30]) the maximum change in temperature (∇T) is only around $10^{\circ}C$. The simulations results shows that DEP chip with a thicker 3D silicon electrode can greatly reduced the change in temperature, hence help in reducing the Joule heating effect during testing. Further simulations are carried out to investigate the thermal effect when increasing the applied voltage. Graphical plot of different voltage versus change in temperature (∇T) for both cases of planar- and 3D-silicon electrode is presented in [30] (the graph was plotted for the point where the maximal temperature is achieved). It is found that when the applied voltage increases, the change of temperature of planar device increases much faster compared to the device with 3D silicon electrode. For example, when the applied voltage is 40V (peak to peak), the temperature rise of planar device is around 40^{O}C while the temperature rise of 3D electrode is only 4 ^{O}C. Effect of different medium electrical conductivity (σ_m) with respect to change in temperature at a fixed applied voltage of 20V peak-to-peak is presented in Figure 9(the graph was plotted for the point where the maximal temperature is achieved). It is observed that device with planar electrode is more sensitive to temperature change with different conductivity as compared to device with 3D silicon electrode. For example, with electrical conductivity set at $0.5Sm^{-1}$, the change in temperature for device with 3D silicon electrode is about $5^{\circ}C$ as compared to around $50^{\circ}C$ for the case of device with planar electrode. These data

show that the change in temperature is 8-10 times lower in device with 3D silicon electrodes as compared to the classical DEP devices with planar electrodes.

4. Testing

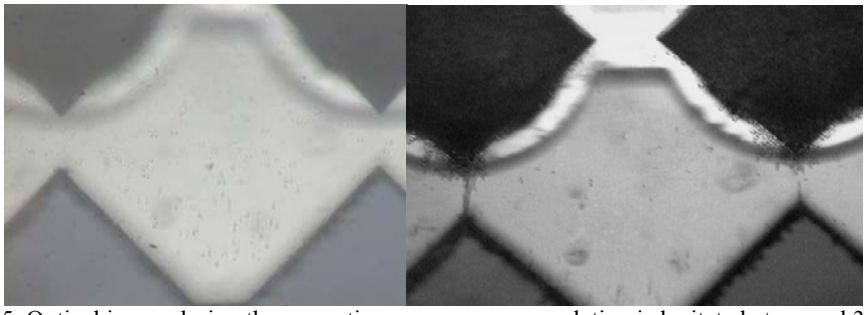

Fig. 5. Optical image during the separation process: one population is levitated at around 30μm from the bottom (a) while the other one is trapped on the bottom of the device by positive DEP (b)

The testing of the working principle was performed using viable and nonviable yeast cells. Yeast cells were incubated and split into two populations: one population was boiled for 10 minutes in a 5mL centrifuge tube with PBS (nonviable cells). Both populations were mixed and resuspended in the separation buffer. The conductivity of the separation buffer was adjusted to about 500 μS/cm using conductivity meter (Oakton 300). The final concentration of the cells was around 5×10^5 cells/mL. The experimental condition for separation was established in a previous work: [16] the applied voltage was 20 V peak-to-peak at a frequency of 20 kHz generated by function generator (HP33250A). The flowing of the solution through the DEP device was performed with a syringe pump (Cole-Parmer 74900 series) through a Teflon tube. Two connectors fabricated by polymer printing machine (OBJET EDEN350) assured the inlet and outlet connections. Separation of the viable and nonviable populations was achieved for flow rate velocities of the fluid around 0.25 mL/min. An optical image taken during the separation process is presented in Figure 5a and Figure 5b by defocusing the microscope. The levitation of the cells that exhibit negative DEP is around 30-35 μm from the bottom of the microfluidic channel (measured using the microscope). Can be noticed that the cells that exhibit negative DEP (figure 5b) are flowing in the vicinity of the thick electrode.

5. Conclusion

To summarize, the paper proposes a field-flow separation method in a DEP device with asymmetric electrodes (one thick, one thin) under continuous flow. The

separation method consists of trapping one population to the bottom of the microfluidic channel using positive DEP, while the other population that exhibits negative DEP is levitated and flowed out. Upon release of the electrical field, the second population can be collected at the outlet in the same manner. Viable and nonviable yeast cells were used for testing the separation method.

REFERENCES

[1]. *R. Pethig, M.S. Talary, R .S. Lee,* "Enhancing travelling-wave dielectrophoresis with signal superposition", IEEE Eng. Med. Biol. Mag., **vol. 22(6)**, (2003) pp. 43-50.

[2]. *L. Cui, D. Holmes and H. Morgan***, "**The dielectrophoretic levitation and separation of latex beads in microchips", Electrophoresis, **vol. 22**, 2001, pp. 3893–3901.

[3]. *E.B. Cummings and A. K. Singh,* "Dielectrophoresis in microchips containing arrays of insulating posts: theoretical and experimental results", Anal. Chem., **vol. 75,** 2003, pp. 4724–4731.

[4]. *C. Iliescu, G.L. Xu, F.C. Loe, P.L. Ong and F.E.H. Tay,* "A 3 dimensional dielectrophoretic filter chip", Electrophoresis, **vol. 28(7)**, 2007, pp. 1107-1114.

[5]. *P.Y. Chiou, A.T. Ohta, M.C. Wu,* Massively parallel manipulation of single cells and microparticles using optical images", Nature, **vol. 436(21)**, 2005, pp. 370-372.

[6]. *C.H. Kua, Y.C. Lam, I. Rodriguez, C. Yang and K.Y. Toumi*, "Dynamic cell fractionation and transportation using moving dielectrophoresis", Anal. Chem. **vol. 79**, 2007, pp. 6975 -6987.

[7]. *S. Masuda, M. Washizu and T. Nanba,* "Novel method for cell fusion in field construction area in fluid integrated circuit", IEEE Trans. on Ind. Applications **vol. 25(4)**, 1989, pp. 732-737.

[8]. *J. Park, B. Kim, S.K. Choi, H. Su, S.H. Lee and K.I. Lee,* "An efficient cell separation system using 3D-asymmetric microelectrodes", Lab Chip **vol. *5***, 2005, pp. 1264–1270.

[9]. *J. Voldman, M. Toner, M.L. Gray and M.A. Schmidt,* "Design and analysis of extruded quadrupolar dielectrophoretic traps", J. Electrostatics, **vol. 57**, 2003, pp. 69-90.

[10]. *B.Y. Park, M. J. Madou,* "3-D electrode designs for flow-through dielectrophoretic systems", Electrophoresis **vol. 26**, 2005, pp. 3745-3757.

[11]. *C. Iliescu, G.L. Xu, V. Samper and F.E.H. Tay,* "Fabrication of a dielectrophoretic chip with 3D silicon electrodes", J. Micromech. Microeng. **vol. 15(3)**, 2005, pp. 494-500.

[12]. *C. Iliescu, L.M. Yu, G.L. Xu and F.E.H. Tay*, "A dielectrophoretic chip with a 3D electric field gradient", J. Microelectromech. Syst., **vol. 15(6),** 2006, pp. 1506-1513.

[13]. *G.H. Markx and R. Pethig*, Dielectrophoretic separation of cells: continuous separation, Biotechnology and Bioengineering, **vol. 45**, 1995, pp. 337-343.

[14]. *D. Holmes, N.G. Green and H. Morgan*, "Microdevices for dielectrophoretic flow-through cell separation", IEEE Eng. Med. Biol. Mag., **vol. 22(6),** 2003, pp. 85-90.

[15]. *L. Gorre-Talini, J.P. Spatz and P. Silberzan*, "Dielectrophoretic ratchets", Chaos, **vol. 8(3)**, 1998, pp. 650-656.

[16]. *C. Iliescu, G. Tresset and G.L. Xu,* "Continuous field-flow separation of particle populations in a dielectrophoretic chip with 3D electrodes", Appl. Phys. Lett. **vol. 90(23),** 2007, pp. 234104.

[17]. *L. Yu, C. Iliescu, G. Xu and F.E.H. Tay,* "Sequential field-flow cell separation method in a dielectrophoretic chip with 3D electrodes", J. Microelectromech. Syst. **vol. 16(5)**, 2007, pp. 1120 -1129.

[18]. *C. Iliescu, L. Yu, F.E.H. Tay and B. Chen,* "Bidirectional field flow particle separation method in a dielectrophoretic chip with 3D electrodes", Sens. Actuators B **vol. 129(1),** 2008, pp. 491 -496.

[19]. *T. Rogers and J. Kowal,* "Selection of glass, anodic bonding conditions and material compatibility for silicon-glass capacitive sensors", Sens. Actuators A, **vol. 46–47,** 1995, pp. 113–120.

[20]. *C. Iliescu, B.T. Chen and J.M. Miao,* "On the wet etching of Pyrex glass", Sens. Actuators A, **vol. 143(1)**, 2008, pp. 154-161.

[21]. *C. Iliescu, J.M. Miao and F.E.H. Tay,* "Optimization of PECVD amorphous silicon process for deep wet etching of Pyrex glass", Surf. Coat. Technol. **vol. 192(1)**, 2005, pp. 43-47.

[22]. *C. Iliescu, J. Miao and F.E.H. Tay,* "Stress control in masking layers for deep wet micromachining of Pyrex glass", Sens. Actuators A 117(2) (2005) 286-292.

[23]. *C. Iliescu, J. Jing, F.E.H. Tay, J. Miao and T.T. Sun*, "Characterization of masking layers for deep wet etching of glass in an improved HF/HCl solution", Surf. Coat. Technol. **vol. 198(1-3),** 2005, pp. 314-318.

[24]. *C. Iliescu, F.E.H. Tay and J. Miao,* "Strategies in deep wet etching of Pyrex glass", Sens. Actuators A **vol. 133(2),** 2007, pp. 395-400.

[25]. *M.P. Hughes,* "Strategies for dielectrophoretic separation in laboratory-on-a-chip systems", Electrophoresis **vol. 23,** 2002, pp. 2569–2582.

[26]. *P.R.C. Gascoyne and J. Vykoukal*, **"**Particle separation by dielectrophoresis", Electrophoresis, **vol. 23**, 2002, pp. 1973–1983.

[27]. *H. Morgan, A.G. Izquierdo, D. Bakewell, N.G. Green and A. Ramos,* "The dielectrophoretic and travelling wave forces for interdigitated electrode arrays: analytical solution using Fourier series", J. Phys. D: Appl. Phys. **vol. 34**, 2001, pp. 1553-1561.

[28]. *R. Pethig, J.P.H. Burt, A. Parton, N. Rizvi, M.S. Talary and J.A. Tame,* "Development of biofactory-on-a-chip technology using excimer laser micromachining", J. Micromech. Microeng. **vol. 8**, 1998, pp. 57-63.

[29]. *J. Kentsch, M. Durr, T. Schnelle, G. Gradl, T. Muller, M. Jager, A. Normann and M. Stelzle*, "Microdevices for separation, accumulation, and analysis of biological micro- and nanoparticles", Proc. IEE Nanobiotechnology, **vol. 150(2)**, 2003, pp. 82-89.

[30]. *F.E.H. Tay, L. Yu, A.J. Pang and C. Iliescu*, "Electrical and thermal characterization of a dielectrophoretic chip with 3D electrodes for cells manipulation", Electrochim. Acta **vol. 52(8)**, 2007, pp. 2862-2868.

[31]. *G.H. Markx, R. Pethig and J. Rousselet,* "The dielectrophoretic levitation of latex beads, with reference to field-flow fractionation", J. Phys. D: Appl. Phys. **vol. 30**, 1997, pp. 2470–2477.

[32]. *C. Iliescu, G.L. Xu, P. L. Ong and K.J. Leck,* "Dielectrophoretic separation of biological samples in a 3D filtering –chip", J. Micromech. Microeng. **vol. 17(7),** 2007, pp. S128-S136

[33]. *C. Iliescu, G. Tresset, G. Xu* "Dielectrophoretic field-flow method for separating particle populations in a chip with asymmetric electrodes", Biomicrofluidics, **vol. 3(4),** 2009, 044104

[34]. *F.S. Iliescu, A.R. Sterian, E. Barbarini, M. Avram, C. Iliescu*, "Continuous separation of white blood cells from blood in a microfluidic device" UPB Scientific Bulletin-Series A-Applied Mathematics and Physics, **vol. 71(4),** 2009, pp. 21-30

[35]. *C. Iliescu, G.L. Xu, E. Barbarini, M. Avram, A. Avram*, "Microfluidic device for continuous magnetophoretic separation of white blood cells" Microsystem Technologies, **vol. 15(8)** 2009, pp. 1157-1162

[36]. *T.B. Jones*, "Electromechanics of particles", Cambridge University Press, 1995.